

# Design of Mechanically Robust High- $T_g$ Polymers: Mechanical Properties of Glassy Poly(ester carbonate)s with Cyclohexylene Rings in the Backbone

Xiangyang Li<sup>†,§</sup> and Albert F. Yee<sup>\*,‡</sup>

Macromolecular Science and Engineering, University of Michigan, Ann Arbor, Michigan 48109, and Materials Science and Engineering, Macromolecular Science and Engineering, University of Michigan, Ann Arbor, Michigan 48109

Received May 26, 2004; Revised Manuscript Received July 20, 2004

**ABSTRACT:** The incorporation of trans cyclohexylene (C-ring) groups into the main chain glassy polymers has been found to increase chain motion. With the increase in trans C-ring content, Young's modulus and yield stress both decrease. A linear correlation among Young's modulus, yield stress, and the inverse of the coefficient of thermal expansion has been found in this work. With the increase in trans C-ring content, post-yield stress drop (PYSD) decreases, the tendency to necking in tensile test decreases, and the activation volume increases. The results are consistent with the idea that thermal expansion, Young's modulus, and yield stress are predominantly controlled by intermolecular forces. Necking and PYSD are related not only to chain stiffness but also closely to polymer chain motion. On the basis of the results, the hypothesis that the incorporation of trans C-ring enhances local segmental motions, which effectively modulates interchain interactions, is proposed.

## 1. Introduction

Main chain segmental motions in polymer glasses have been proposed to play a crucial role in their mechanical properties, such as yield stress, craze stress, and impact strength;<sup>1–4</sup> it has been further proposed that these molecular motions can be enhanced by conformational transitions in the main chain, such as the ring inversion of cyclohexylene (C-ring).<sup>2–5</sup> In previous papers,<sup>6,7</sup> the synthesis, characterization, secondary relaxation behavior, and physical properties of three series of high- $T_g$  glassy polymers with the incorporation of main chain C-rings have been reported. The chemical structures of these polymers are shown in Figure (1), and their  $T_g$ s are listed in Table (1). In this paper, the effects of main chain C-ring incorporation on some mechanical properties, such as Young's modulus, yield stress, and post-yield stress drop (PYSD), are reported.

Conventional efforts to design and synthesize high- $T_g$  polymers often result in compromised mechanical properties. For example, by introducing two methyl groups ortho to the carbonate group of BPA-PC, tetramethyl bisphenol A polycarbonate (TMBPA-PC) is obtained with a  $T_g$  of 200 °C;<sup>8</sup> by replacing BPA with SBI, a polycarbonate (SBI-PC) with  $T_g$  of 230 °C is produced<sup>9</sup> (for structures see Figure 2). But these two polymers are extremely brittle at room temperature. A common feature of these two polymers is that they are both restricted in the types of possible local molecular motions. In SBI-PC, SBI is locked into a twisted bulky banana shape, and SBI-PC has a very limited, confined local motion.<sup>6</sup> In TMBPA-PC, the local motion is restricted by the steric interaction between the carbonate groups and their ortho methyl groups.<sup>10</sup> By contrast,

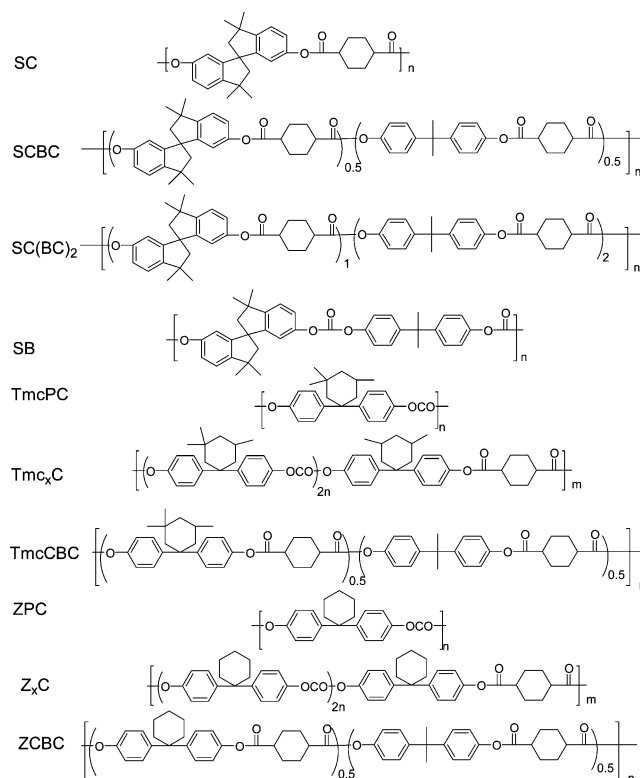


**Figure 1.** Chemical structures and short names for all the polycarbonates, polyesters, and poly(ester carbonate)s.

TmcPC has a high  $T_g$  of 240 °C, but its mechanical properties are comparable to those of BPA-PC.<sup>11</sup> The motions are also restricted in TmcPC by the severe steric hindrance between the axial methyl group and the axial phenyl ring, but motions of the carbonate group are not restricted.<sup>6</sup> These examples point out the very important influence of molecular motions on mechanical properties.

<sup>†</sup> Macromolecular Science and Engineering.

<sup>‡</sup> Materials Science and Engineering, Macromolecular Science and Engineering.

<sup>§</sup> Current address: Lexan Technology, GE Advanced Materials, Mount Vernon, IN 47620.

\* Corresponding author: e-mail afyee@uci.edu.

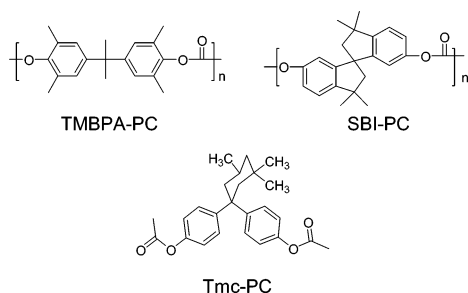


**Figure 2.** Chemical structures of TMBPA-PC, SBI-PC, and TmcPC.

**Table 1. Molecular Weight and Glass Transition Temperature of the Polymers**

polymer	$M_n$	$M_w$	$T_g/^\circ\text{C}$
SC	51K	778K	275
SCBC	39K	77K	246
SB	126K	262K	198
TmcPC	106K	204K	240
Tmc <sub>5</sub> C	80K	137K	245
Tmc <sub>3</sub> C	75K	119K	252
Tmc <sub>1</sub> C	40K	84K	283
TmcCBC	66K	131K	257
ZPC	32K	79K	182
Z <sub>5</sub> C	92K	164K	190
Z <sub>3</sub> C	63K	109K	195
Z <sub>1</sub> C	52K	111K	228
ZCBC	87K	171K	220

Yielding and crazing are the two principal modes of irreversible deformation in thermoplastics. Brittle failure is often associated with crazing while ductile failure is associated with shear yielding. If the craze stress in a given stress state is higher than the yield stress, then yielding will be the preferred form of deformation, and the material will fail in a ductile manner.

Phenomenologically, yielding is temperature and rate dependent and can be described as a nonlinear stress relaxation process in response to a large imposed strain or their conjugate set in creep and imposed stress. However, despite extensive research activities in this area, there is still not a generally accepted model of the molecular mechanism of yield. Different molecular models have been proposed to explain the yield process. These include Eyring's state transition model,<sup>12</sup> Robertson's conformational change model,<sup>13</sup> Argon's dislocation model,<sup>14</sup> and others. A detailed review of molecular models on yielding was given by Crist<sup>15</sup> and Stachurski.<sup>16</sup> All the models enjoy some success in explaining and fitting experimental results. Among these, the Eyring model is the most general and the most successful, but perhaps because it lacks molecular detail. Robertson's model emphasizes intramolecular interactions, whereas Argon's model emphasizes intermolecular interactions.

The Eyring equation can be represented in a simplified form as

$$\frac{\sigma_y}{T} = \frac{\Delta H}{vT} + \frac{R}{v} \ln \frac{2\dot{\epsilon}}{\dot{\epsilon}_0} \quad (1)$$

where  $\dot{\epsilon}$  is the strain rate,  $\dot{\epsilon}_0$  a constant preexponential factor,  $v$  the activation volume for the molecular event,  $\sigma_y$  the yield stress,  $R$  the gas constant, and  $T$  the absolute temperature. Thus, plots of  $\sigma_y/T$  vs  $\ln \dot{\epsilon}$  should give a series of parallel, straight isotherms from which the activation energy  $\Delta H$  and activation volume  $v$  can be extracted. Eyring's equation describes the relation-

ship between yield stress and activated molecular motions. The scale of the molecular motions can be described by the activation volume  $v$ .  $v$  is defined as the volume swept out by the chain or chain segments during their flip or climb over the potential energy barrier. Previous research results indicate that this volume is much larger than the sizes of Kuhn segment of various polymers. Haward and Thackray<sup>17</sup> showed that the Eyring flow volumes varied from 2 to 10 times those of the "statistical links" in a series of polymers. The statistical link is the same as the Kuhn length, which is indicative of the segment size of the polymer chain, which in turn is equivalent to a freely jointed chain in determining the overall configuration in dilute solution. The result suggests that the yield process involves the cooperative motions of a larger number of chain segments than would be required for conformational change in dilute solution. In the glassy state, since each polymer chain is surrounded and interpenetrated by other polymer chains, it is not physically possible for Eyring's flow volume to be caused by the movement of segments from a single chain; instead, it must involve some collection of segments from neighboring chains.

A correlation between activation volume  $v$  and the scale of molecular motion at yield was given by Chen and Yee<sup>2</sup> and by Liu and Yee.<sup>4</sup> Chen and Yee<sup>2</sup> studied structurally similar polyesters while Liu and Yee<sup>4</sup> studied structurally similar poly(ester carbonate)s. They observed that as the activation volume increased, the yield stress dropped. The increased activation volume was interpreted as an increase in the scale of polymer chain motions, which could relax stress more effectively, thus facilitating the yielding process. A more direct correlation between the scale of molecular motion and yielding process was given by Xiao et al.<sup>1</sup> By systematic chemical modification of their polymer structures, they tailored different scales of molecular motion which were observable by DMA. They found that when the scale of in-chain cooperative motion was small, a higher temperature was needed to activate the copolymer to yield; when the scale was large, the brittle to ductile transition temperature shifted to a much lower temperature.

Even though the activation volume cannot be correlated with the scale of molecular motion at yield for all polymers, the above discussion demonstrates that it is possible to make this correlation for at least a family of polymers whose structures are systematically varied through chemical modification.

## 2. Experimental Section

Tensile tests were performed on dog-bone-shaped polymer films prepared from polymers shown in Figure 1. The films were prepared from dry polymer powders dissolved in dichloromethane, forming 5% solutions. The solution was filtered through a microfilter and cast on clean glass slides. The solvent was evaporated slowly at room temperature overnight. The films were then floated off the glass slides with distilled water. They were placed under vacuum at 65 °C for 48 h to remove residual solvent. No further heat treatment was applied prior to the tensile tests. Because the temperature used to drive off the residual solvent was at least 150 °C lower than the glass transition temperature for most of the polymers, physical aging effect can be assumed to be negligible. All the films were visually clear and were confirmed to be amorphous by DSC. The polymer film was cut by a custom-made stainless steel cutter into dog-bone-shaped test specimens with thickness of 0.1 mm. The shape and dimensions of the specimen are shown in Figure 3.

The strain rate dependence of yield stress at 25 °C for the polymers studied in this paper was determined by a series of

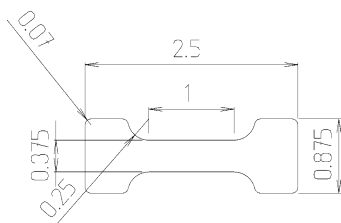


**Figure 3.** Geometry of the dog-bone-shaped specimen, units in inches.

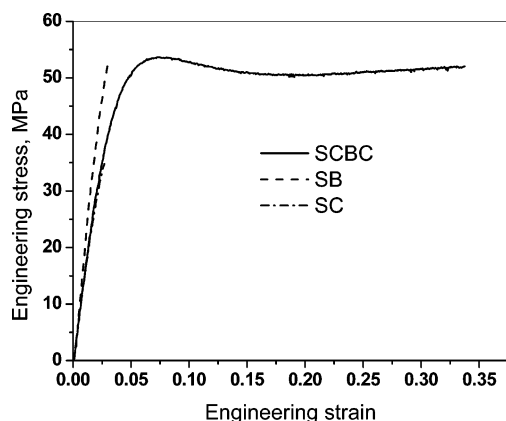


**Figure 4.** Tensile behavior of SCBC, SB, and SC at a strain rate of  $2.1 \times 10^{-2} \text{ s}^{-1}$ ;  $T = 25^\circ \text{C}$ .

tensile tests with a screw-driven testing machine (Instron 4502). The nominal yield stresses are reported as averages from no fewer than three duplicate tests. Since attaching an extensometer on a film is not feasible, the engineering strains were obtained through a calibration procedure. The calibration experiment was performed on a SCBC specimen and a video camera. The specimen had gauge marks millimeters apart. An experiment session—pulling the specimen in tension—was videotaped and played back to measure displacements in the gauge section. The grip separation was the same as the crosshead displacement and was used to calculate the apparent strain. An apparent strain  $\epsilon'$  was calculated by dividing the displacement in grip separation ( $\Delta L$ ) by the original grip separation ( $L_0$ ). An engineering strain ( $\epsilon$ ) was calculated from dividing the displacement in the gauge section ( $\Delta l$ ) by the original gauge length ( $l_0$ ). By plotting the engineering strain against the apparent strain, a calibration was obtained. Only the linear portion of the data set was used to set up the calibration factor. Since this calibration factor was used to compensate for deformations outside the gauge section, the reasonable assumption was made that, in the elastic range, the ratio of the deformation in the gauge section to the overall deformation was constant. This method was found to be reproducible and showed little dependence on the strain rate and was thus applied to all polymers at all strain rates.<sup>1,18</sup>

The coefficients of thermal expansion of all the polymers have been reported previously.<sup>7</sup>

### 3. Results and Discussion

**3.1. Yielding.** SBI-PC is extremely brittle.<sup>9</sup> By incorporating main chain C-rings to induce some motion, it had been hoped that the polymers could be made ductile. But the polymers with C-ring mole fraction up to 0.5 failed to behave in a ductile manner. Shown in Figure 4 is the tensile behavior of SC, SB, and SCBC. Both SC and SB fail in a brittle manner, whereas SCBC is ductile. In a previous paper,<sup>6</sup> it had been concluded that the C-ring inversion is still active in SC. From its brittleness in tension, it can be reasonably deduced that the C-ring inversion is not able to impart much motion

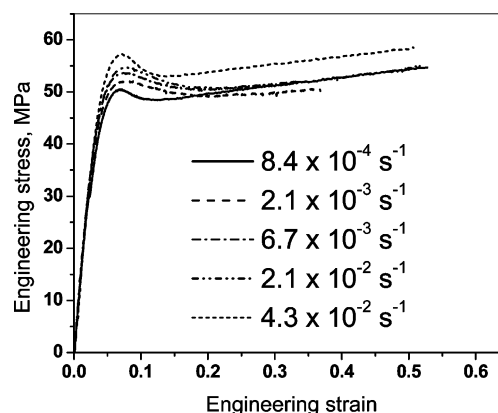


**Figure 5.** Tensile behavior of SCBC at different strain rates;  $T = 25^\circ \text{C}$ .

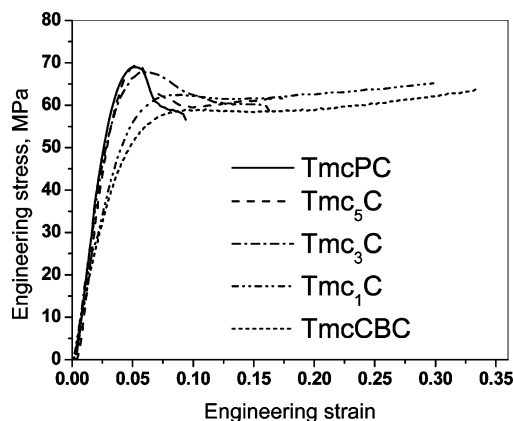


**Figure 6.** Tensile behavior of Tmc polymers at a strain rate of  $2.1 \times 10^{-2} \text{ s}^{-1}$ ;  $T = 25^\circ \text{C}$ .

to its bulky neighbor, SBI. Thus, it can be deduced that, overall, any backbone motion is still quite localized. Apparently, the motions from carbonate groups, BPA moieties, and the combination of these two entities similarly fail to impart much motion to SBI; therefore SB is brittle. Interestingly, SCBC is capable of undergoing plastic deformation at different strain rates ranging from  $8.4 \times 10^{-4}$  to  $4.3 \times 10^{-2} \text{ s}^{-1}$ , as shown in Figure 5. In SCBC, on a single polymer chain, between every two SBI moieties, there is, on average, a CBC segment. From DMA results, the characteristic C-ring inversion is shown to be active in SCBC, and its ductile behavior suggests the strong possibility that cooperative segmental motion takes place in a CBC segment. This segmental motion apparently provides a “softer” environment to SBI entities and may even facilitate their motion to such an extent that plastic flow can take place when a sufficiently high stress is applied. The molecular mechanism involved is still not clear, but by comparison with SC and SB, where a single C-ring unit or a BPA unit alone does not provide sufficient motion to facilitate the yield process, it can be surmised that the CBC segmental motion plays a crucial role in whether plastic deformation in shear is possible.

Figure 6 and Figure 7 show the tensile behavior of polymers based on Tmc and BPAZ. Both figures show that with the increase in main chain C-ring content yield stress drops. This change is seen more clearly in Figure 8. Also, with the increase in main chain C-ring concentration, Young's modulus drops as shown in Figure 9. By contrast, a plot of the yield stress or Young's modulus vs total C-ring concentration in Figure

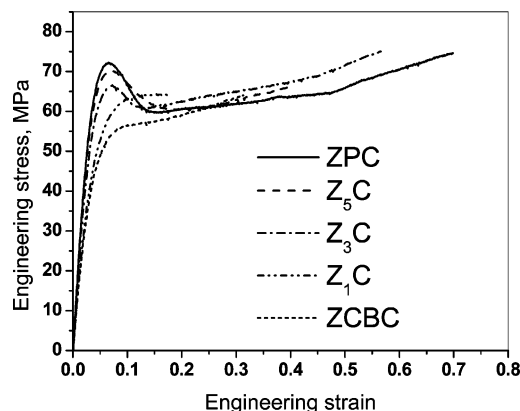


**Figure 7.** Tensile behavior of BPAZ polymers at a strain rate of  $2.1 \times 10^{-2} \text{ s}^{-1}$ ;  $T = 25^\circ \text{C}$ .

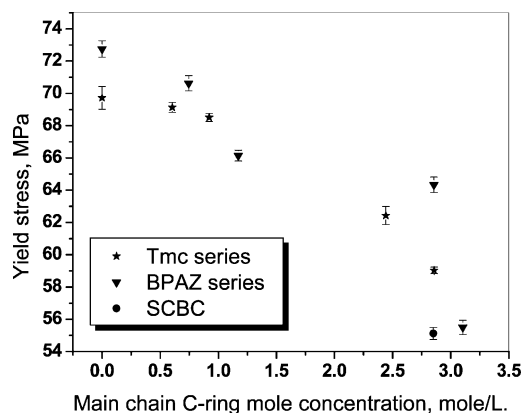


**Figure 8.** Change in yield stress with the change in main chain C-ring concentration;  $T = 25^\circ \text{C}$ .

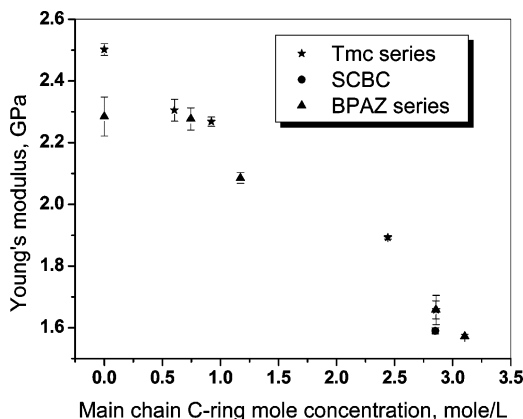


**Figure 9.** Change in Young's modulus with the change in main chain C-ring concentration at a strain rate of  $2.1 \times 10^{-2} \text{ s}^{-1}$ ;  $T = 25^\circ \text{C}$ .

10 shows there is no correlation. This suggests that the change in yield stress or Young's modulus is mainly determined by the change in main chain C-ring content, not by the total C-ring content. This observation is similar to that on the change in thermal expansion<sup>7</sup> and obviously different from that on the secondary relaxation strength.<sup>6</sup> The similarity in the dependences of thermal expansion, yield stress, and Young's modulus on the change in main chain C-ring concentration indicates that they have similar molecular origins.

**3.2. Yield Stress and Young's Modulus.** Figure 11 shows there is a linear correlation between Young's modulus and the inverse of linear thermal expansion coefficient at  $25^\circ \text{C}$  for all the polymers studied. Inter-

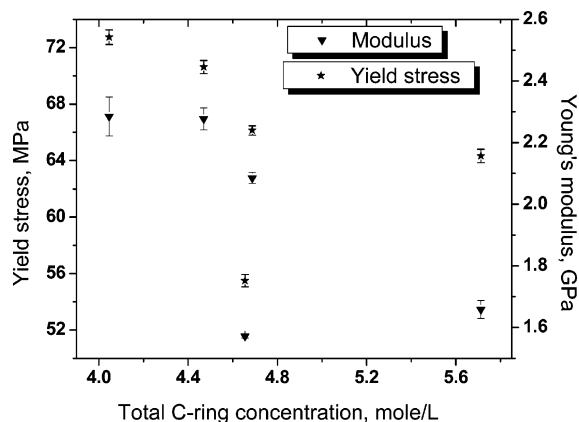


**Figure 10.** Change in yield stress and Young's modulus with the change in total C-ring concentration for BPAZ polymers at a strain rate of  $2.1 \times 10^{-2} \text{ s}^{-1}$ ;  $T = 25^\circ \text{C}$ .

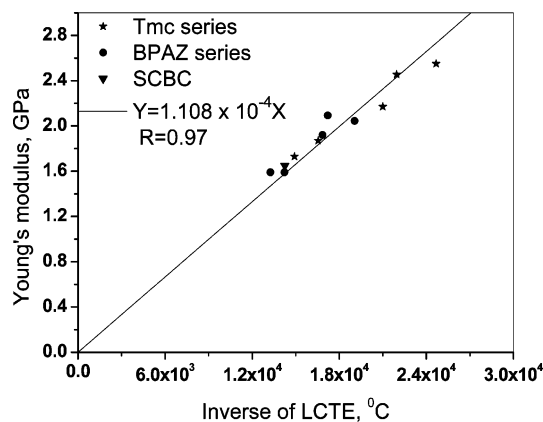


**Figure 11.** Correlation between Young's modulus and the inverse of LCTE; strain rate is  $2.1 \times 10^{-2} \text{ s}^{-1}$ ;  $T = 25^\circ \text{C}$ .

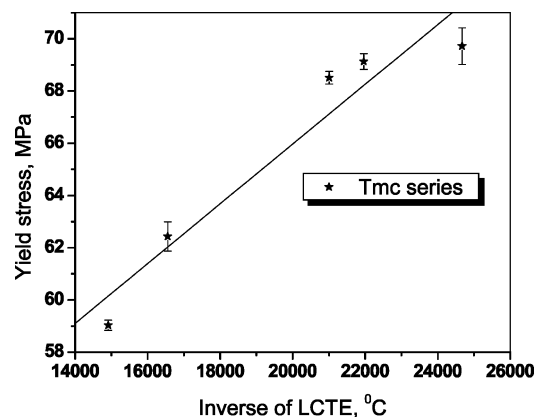


**Figure 12.** Correlation between yield stress and the inverse of LCTE for Tmc polymers; strain rate is  $2.1 \times 10^{-2} \text{ s}^{-1}$ ;  $T = 25^\circ \text{C}$ .

estingly, there is also a near linear correlation between yield stress and the inverse of LCTE as shown in Figure 12 and Figure 13. These correlations imply that there should be a near linear correlation between yield stress and Young's modulus, which is indeed observed in Figure 14.

As discussed previously,<sup>7</sup> thermal expansion is mainly the expansion of the distance between polymer chains, since the expansion of the primary covalent bonds is, by comparison, negligible. Therefore, thermal expansion is controlled by intermolecular potentials. Young's modulus for glassy polymers is in the range of GPa, similar to that of polymer crystals in the direction



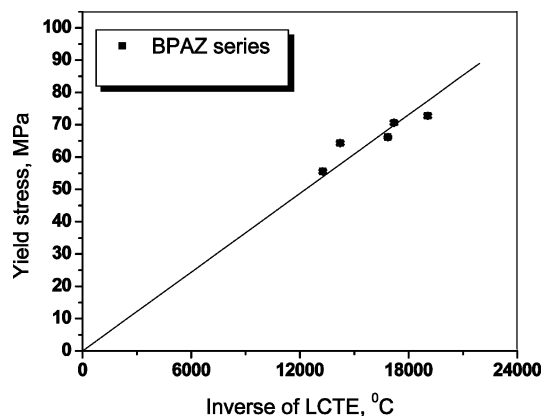


**Figure 13.** Correlation between yield stress and the inverse of LCTE for BPAZ polymers; strain rate is  $2.1 \times 10^{-2} \text{ s}^{-1}$ ,  $T = 25^\circ \text{C}$ .

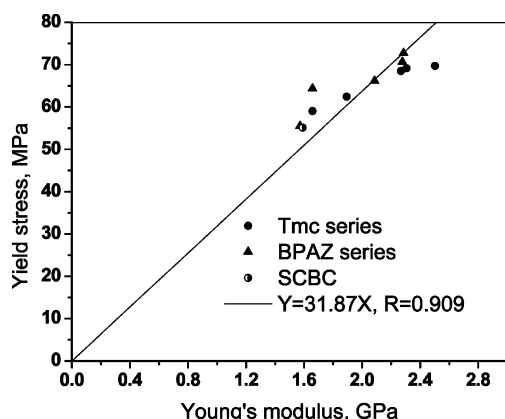


**Figure 14.** Correlation between Young's modulus and yield stress at a strain rate of  $2.1 \times 10^{-2} \text{ s}^{-1}$ ;  $T = 25^\circ \text{C}$ .

perpendicular to the chain directions, which is far less than 100 GPa, the value for typical polymer crystals along the chain direction.<sup>19</sup> The similarity in Young's moduli for glassy polymers and polymer crystals in the transverse directions indicates that intermolecular interaction controls the elastic deformation in polymer glasses. Therefore, the linear correlation between elastic modulus and the inverse of thermal expansion coefficient is simply a natural manifestation of the reasonable conclusion that the same interchain interaction governs their behaviors.

The near linear correlation between Young's modulus and yield stress suggests that interchain interaction also dominates the yielding process. In this sense, this phenomenon is in accord with Argon's model for plastic deformation.<sup>14</sup> In this model, the plastic deformation is assumed to be a process wherein chain segments, driven by external stress, overcome intermolecular interactions. Yang found, in her molecular dynamic simulation of the deformation of amorphous polyethylene, that the strain energy from Lennard-Jones potential dominates the total strain energy as shown in Figure 15.<sup>20</sup> A similar result was observed by Fan, who found in his molecular mechanics study of the yielding of glassy polycarbonate<sup>21</sup> that the maximum of the derivative of total strain energy with strain gives the yield stress. Therefore, in this sense, yield stress is also governed mainly by interchain interactions. The linear correlation between Young's modulus and yield stress has been reported by many researchers.<sup>22–24</sup> This observation may lead to the conclusion that interchain

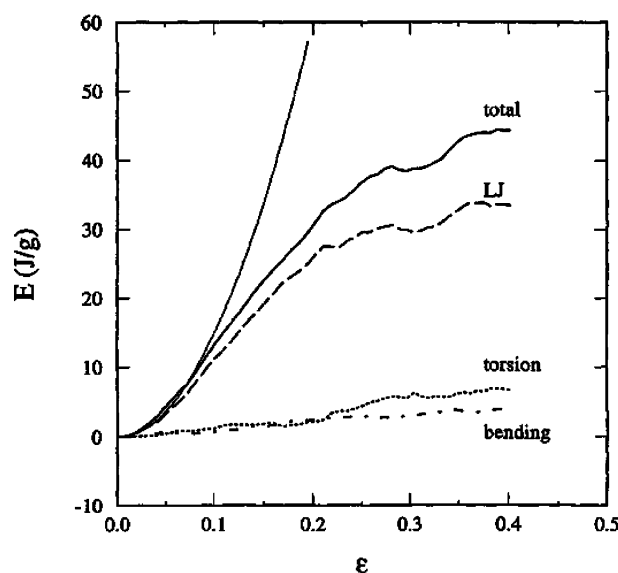


**Figure 15.** Average bending, torsional, nonbonded Lennard-Jones, and total internal energies vs strain during tensile tests at 100 K. The thin solid line indicates how the energy of the system would evolve with strain if the deformation was purely elastic.<sup>20</sup>

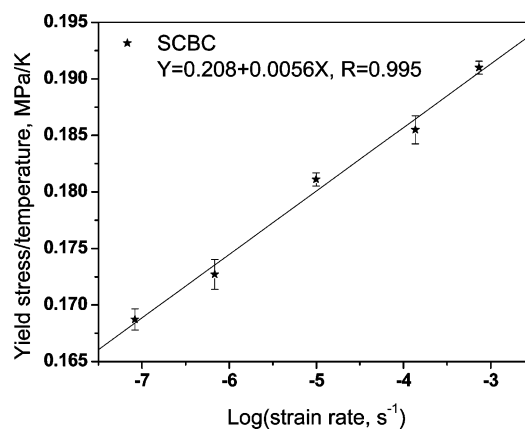


**Figure 16.** Yield stress vs log strain rate plot at  $25^\circ \text{C}$  for SCBC.

interaction is the sole factor controlling the yielding process. Numerically this seems to be correct, but stating so underestimates the effect of intrachain interaction on interchain forces. As discussed previously,<sup>7</sup> the incorporation of main chain C-rings in the polymers studied here leads to enhanced in-chain segmental motion. These motions, especially the fast flip-flop motion of main chain C-rings, probably modify the interchain interaction through decreasing the effective contact areas and interacting times. As a result, the intrachain motion modulates the interchain interaction. This modulation effect is most effective through main chain segmental motion, as demonstrated by the remarkably good correlation between LCTE, yield stress, Young's modulus, and the main chain C-ring concentration instead of total C-ring concentration (including side chain C-rings).

**3.3. Activation Volume and Post-Yield Stress Drop.** The log strain rate dependence of yield stress at room temperature for all the polymers follows quite well the Eyring equation as shown in Figures 16–18. From the slope of the Eyring plot, the activation volume for the yielding process can be calculated. Figure 19 and Figure 20 show that in both Tmc and BPAZ polymers

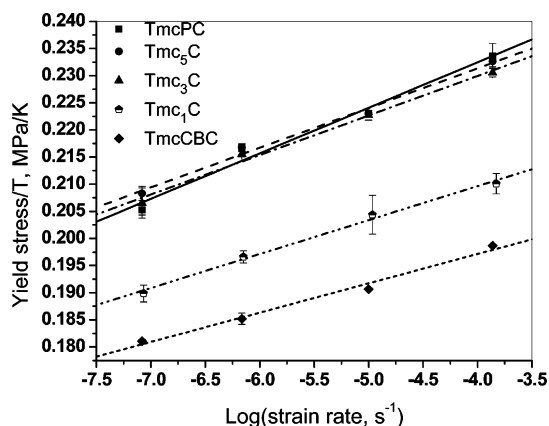


**Figure 17.** Yield stress vs log strain rate plot at 25 °C for Tmc polymers.

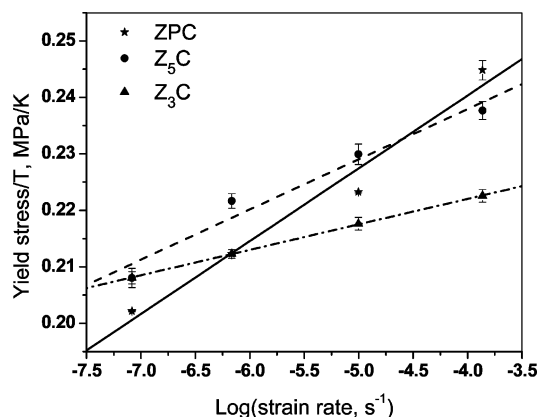


**Figure 18.** Yield stress vs log strain rate plot at 25 °C for BPAZ polymers.

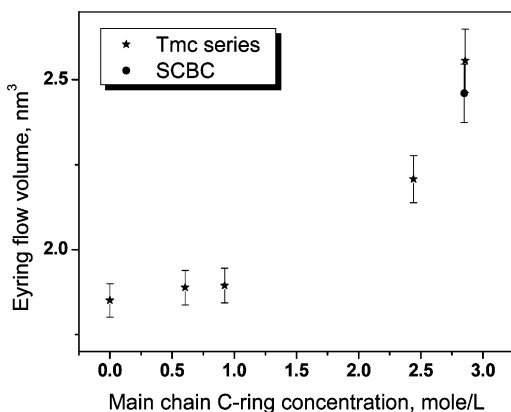


**Figure 19.** Eyring flow volume for Tmc polymers and SCBC at 25 °C.

the Eyring flow volume increases with the increase in main chain C-ring concentration. This means more molecular segments are involved in the yield process as more main chain C-rings are incorporated. As discussed in a previous paper,<sup>7</sup> the main chain C-ring inversion may require large-scale reorientation of its neighbors; thus, this cooperative motion is probably more effective in dispersing strain energy. The denser this cooperative motion is in the system, the easier it is for the local stress to be relieved by distributing it among other polymer chains. SBI has the same molecular weight as Tmc; the former is severely restricted in the freedom of motion because of its locked configuration, while the latter has restricted motion due to the

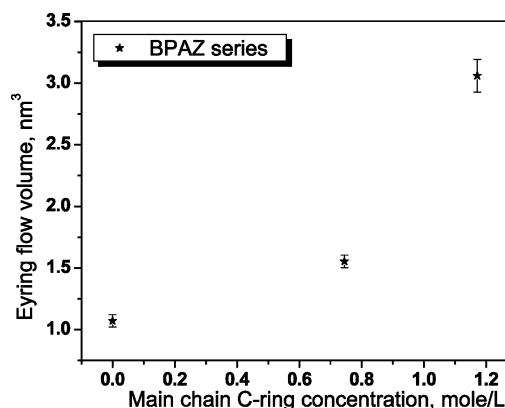


**Figure 20.** Eyring flow volume for BPAZ polymers at 25 °C.

steric interaction between the axial phenyl group and the axial methyl group. Interestingly, TmcCBC and SCBC have basically the same  $T_g$ , very similar LCTE, and mechanical properties. Figure 19 shows that SCBC has a similar activation volume to that of TmcCBC. This, in a sense, is remarkable because in the external thermal or stress field TmcCBC and SCBC respond similarly despite their inherent differences in mobility. This suggests that in SCBC the mobility of SBI, which is very similar to that of Tmc, is probably mobilized by the cooperative motion of CBC segments.

In most engineering stress vs engineering strain plots for ductile polymers, a post-yield stress drop (PYSD) is observed; this phenomenon is shown in Figure 21. It is due to strain softening and is usually accompanied by necking in tensile tests. Vincent proposed that strain softening was a geometric effect.<sup>25</sup> Brown and Ward found that in most cases there was clear evidence for the existence of an intrinsic yield drop, i.e., a fall in true stress (true strain softening).<sup>26</sup> True strain softening was shown in video-controlled tensile tests<sup>38</sup> and a uniaxial compression test.<sup>39</sup> In most cases, amorphous glasses display true strain softening if they are ductile.<sup>40</sup> From Considere analysis, it can be easily shown a material with true strain softening will exhibit PYSD in tensile test. So the observed PYSD can be a combination of intrinsic material property as well as geometric effect.

As shown in Figures 6 and 7, all the polymers studied here exhibit PYSD except  $Z_1C$  and ZCBC, while it (PYSD) is barely noticeable for Tmc1C and TmcCBC. Except for  $Z_1C$ , ZCBC, Tmc<sub>1</sub>C, and TmcCBC, all other polymers exhibit readily visible necking. It is interesting to discover why these differences exist under the same tensile test conditions.

Necking is due to strain localization. The tendency for glassy polymers to undergo localized plastic deformation (necking) or diffuse deformation was correlated with the "natural hinge length"  $\bar{l}$  of a group of polyimides by Argon and Bessonov.<sup>27</sup> The chemical structures of the polymers they studied are listed in Figure 22. For the four polyimides, it was observed that as the natural hinge length increased, the tendency for necking decreased (Figure 23). Kapton had the highest  $\bar{l}$ , did not neck, and exhibited very diffusive plastic yielding. It was hypothesized by these authors that "plastic flow in glassy polymers is of a highly local nature, but tends to become less so as the natural hinge spacing on molecules increases."

Along a similar line of reasoning, the effect of persistence length on yielding behavior was studied by Ha-

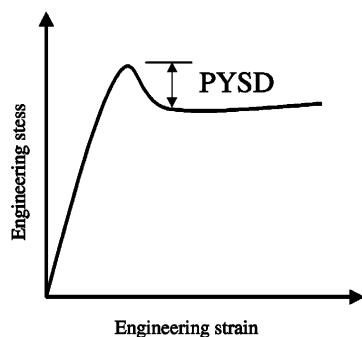


**Figure 21.** Representation of stress-strain curve showing post-yield stress drop (PYSD).

ward et al., who changed the length of stiff chain segments in a series of poly(ester carbonate)s.<sup>28</sup> The series consisted of poly(ester carbonate)s synthesized from bisphenol A and terephthaloyl/isophthaloyl entities (Figure 24). The phthalate ester can be either terephthalate or isophthalate. By changing the ester block length  $n$  or the type of phthalate ester group, the length of chain stiff segment can be changed. For ester block length  $n$  of 4, it was observed that if the phthalate group was terephthalate, the poly(ester carbonate) did not exhibit necking or strain softening, whereas if the phthalate group was isophthalate, the polymer necked and exhibited post-yield stress drop. The latter had a smaller stiff segment length (persistence length) due to a kink introduced by isophthalate, while the former polymer had a larger stiff segment length. It was argued that the observed difference was due to different amounts of strain hardening: in poly(ester carbonate) with terephthalate groups, the chain was more extended, and strain hardening set in earlier than in the polymers with isophthalate groups, where it had a less extended chain configuration. It was also shown by Haward<sup>41</sup> that when the ratio of yield stress to the strain hardening modulus is less than 3, a polymer will deform uniformly. In the

case that this ratio is greater than 3, necking will tend to occur. From this argument, polymer chains with large persistence length are conducive to strain hardening, therefore decreasing the tendency to necking.

Further support for Haward's hypothesis came from two sets of experimental results. First, polyisocyanates were reported to have a very large persistence length and always exhibited uniform deformation.<sup>28</sup> Second, based on a molecular dynamics simulation of Brown and Clarke,<sup>29</sup> the effect of chain configurations on the stress-strain behavior of glassy polymers was studied by McKechnie et al.<sup>30</sup> Different configurations of polyethylene-like polymers with different persistence lengths and trans concentrations were modeled. Then these polymers were subject to tension. It was found that polymers with higher persistence length or higher trans content have more strain hardening. Since these polymers have the same chemical structures, the results are less ambiguous, and the effect of chain stiffness on stress-strain behavior is obvious.

The present results do not contradict the results of either Argon and Bessonov<sup>27</sup> or Haward et al.<sup>28</sup> In the current case, with the incorporation of main chain trans C-rings, the polymer chains are extended, resulting in an increase in the persistence length,<sup>7</sup> and the polymers are found to have a greater tendency to undergo plastic deformation diffusively instead of locally. Furthermore, with the incorporation of main chain trans C-rings, the yield stress drops which will help to lower the ratio of yield stress to the strain hardening modulus, therefore a less tendency to necking. In both Tmc and BPAZ polymers, with the increase in main chain C-ring incorporation, post-yield stress drop decreases; in Tmc1C, Tmc-CBC, Z1C, and ZCBC, PYSD does not occur (Figure 25).

Although there is apparent correlation between chain stiffness and the tendency to diffusive plastic deformation, the strain hardening explanation by Haward et al.<sup>28</sup> may not be the primary reason. Hints to the

No	Polymer	Monomer unit	$T_g, ^\circ\text{C}$	$a_0, 10^{-10}\text{m}$	$\bar{l}, 10^{-10}\text{m}$	$\bar{l}/a_0$
1	Kapton(PM)		>350(*)	2.82	18.0(**)	6.4
2	DFO		270	2.94	11.5(**)	3.9
3	H-H		230	---	8.6	~3.0
4	R-R		200	---	8.1	~2.8
5	PPO		170	3.36	5.6(**)	1.7
6	PC		150	3.09	2.8	0.9
7	PET		65	2.84	2.15	0.8
8	PS		100	4.63	1.55(**)	0.35
9	PMMA		110	2.85	1.55(**)	0.55
	* No true glass transition					
	** Exactly equal to the length of stiff units on the chain					

**Figure 22.** Chemical structures and physical properties of glassy polyimides and some previously investigated glassy polymers.<sup>27</sup>

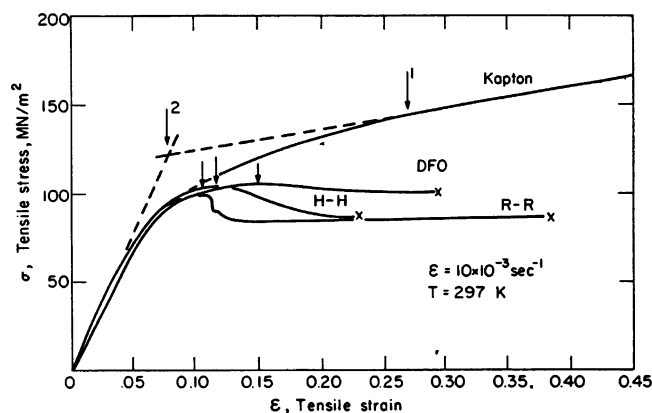


**Figure 23.** Engineering stress–strain curves in tension for the four polyimide films tested. Arrows show positions where yield stresses were evaluated. Crosses show strains where fracture has occurred.<sup>27</sup>

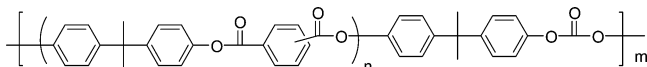


**Figure 24.** Structures of poly(ester carbonate)s studied by Haward et al.<sup>28</sup>

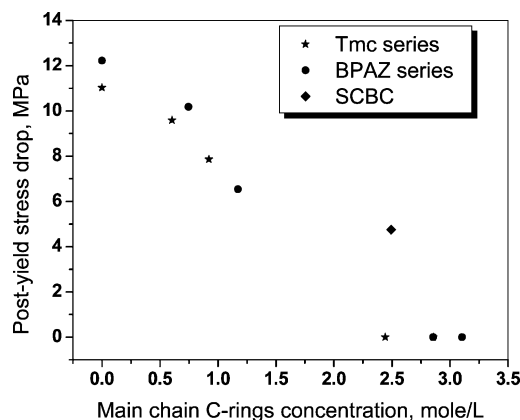


**Figure 25.** Post-yield stress drop vs main chain C-ring concentration.

existence of other reasons come from the stress–strain behavior of aged amorphous polymers. PVC quenched from 90 °C shows hardly any necking or PYSD, but annealed PVC shows prominent necking and PYSD.<sup>28</sup> This behavior was also observed in amorphous poly(ether ether ketone)<sup>31,32</sup> and in amorphous poly(ethylene terephthalate).<sup>33</sup> In all these polymers, physically aged specimens below  $T_g$  exhibit increased yield stress and increased post-yield stress drop compared with those of quenched specimens. There are some reports of the effect of annealing on chain conformational change. Ito et al. proposed that physical aging of amorphous poly(ethylene terephthalate) results in a decrease in the amount of trans conformation relative to gauche conformation based on their IR results.<sup>34</sup> However, Garcia reported no change in the relative concentration of trans vs gauche conformations with annealing of glassy PET in his more recent FTIR measurements.<sup>35</sup> According to Bubeck and Bales,<sup>36</sup> there was no radical change in molecular conformation associated with physical aging. Therefore, from the available data on the effect of annealing on chain conformation, a correlation between PYSD and chain stiffness cannot be deduced. Furthermore, the physically aged and quenched samples of the same material display identical true stress–strain

behavior at large strain levels (therefore identical strain hardening behavior), but they can have different PYSD behavior.<sup>42</sup> So the yield process seems to be more relevant to PYSD.

On the basis of these observations associated with physical aging, the tendency to uniform plastic deformation can be proposed to be closely related with the nature of the dynamics of segmental motions. Physical aging results in slowed-down segmental mobility, i.e., longer relaxation times,<sup>37</sup> so the stress cannot be delocalized to other segments as quickly. Also, physical aging densifies polymers and reduces the average chain spacing. Both effects lead to increased intermolecular forces, which according to our previous arguments lead to higher resistance to plastic deformation, therefore higher yield stress, as confirmed experimentally. In the current polymers, with the increased concentration of main chain C-rings, the thermal expansivity is increased, which is indicative of an increase in the volume fluctuation occupied by each molecular segment. When an external stress is imposed, the ensemble of molecules responds by lowering its internal energy via molecular rearrangements. The more chain motion, the faster the stress can be relaxed, and the lesser the chance for strain localization. This is also in accord with what was found in this work in terms of activation volume. With the increase in main chain C-ring content, the activation volume for yield also increases, which means more chain segments are involved in relaxing the external stress. This is obviously more effective than localized chain motions.

#### 4. Summary

In this paper, it has been shown that with the increased incorporation of main chain C-rings yield stress and Young's modulus both decrease, while the activation volume and the tendency for undergoing uniform deformation both increase. Yield stress and Young's modulus do not have a good correlation with the total C-ring concentration (including side chain C-rings). Main chain C-ring inversion involves larger scale segmental motion, which results in enhanced chain motion. The intrachain polymer motion reduces the interaction area and contact time between polymer chains, resulting in reduced frictional force between polymer chains and therefore reduced resistance to plastic flow. Also, the enhanced chain dynamics can relax imposed external stress faster and more effectively, which results in a lessened tendency to strain localization.

The near linear correlation between yield stress and Young's modulus and the linear correlation between the latter with the inverse of thermal expansion coefficient indicate they all are mainly governed by the relatively weak intermolecular potentials. But overemphasizing this will underestimate the effect of intrachain molecular motion on interchain molecular interaction. Both kinds of interaction need to be taken into account in discussing any physical and mechanical properties: Interchain interaction dictates the thermal expansion coefficient, yield stress, and Young's modulus, while intrachain interaction acts on these properties through modifying the interchain potentials.

**Acknowledgment.** Financial support from the U.S. Air Force Office of Scientific Research (AFOSR) (Grant F49620-98-1-0158) is gratefully acknowledged. The



authors thank one of the reviewers for helpful comments regarding necking and PYSD.

## References and Notes

- (1) Xiao, C. D.; Jho, J. Y.; Yee, A. F. *Macromolecules* **1994**, *27*, 2761–2768.
- (2) Chen, L. P.; Yee, A. F.; Moskala, E. J. *Macromolecules* **1999**, *18*, 5944–5955.
- (3) Liu, J. W.; Yee, A. F. *Macromolecules* **1998**, *31*, 7865–7870.
- (4) Liu, J. W.; Yee, A. F. *Macromolecules* **2000**, *33*, 1338–1344.
- (5) Chen, L. P.; Yee, A. F.; Goetz, J. M.; Schaefer, J. *Macromolecules* **1998**, *31*, 5371–5382.
- (6) Li, X. Y.; Yee, A. F. *Macromolecules* **2003**, *36*, 9411–9420.
- (7) Li, X. Y.; Yee, A. F. *Macromolecules* **2003**, *36*, 9421–9429.
- (8) Freitag, D.; Grigo, U.; Muller, P. R.; Nouvertne, W. *Encycl. Polym. Sci.* **1988**, *11*, 650–719.
- (9) Stueben, K. C. *J. Polym. Sci., Part A* **1965**, *3*, 3209–3217.
- (10) Yee, A. F.; Smith, S. A. *Macromolecules* **1981**, *14*, 54–64.
- (11) Freitag, D.; Fengler, G.; Morbitzer, L. *Angew. Chem., Int. Ed. Engl.* **1991**, *30*, 1598–1610.
- (12) Eyring, H. *J. Chem. Phys.* **1936**, *4*, 283–291.
- (13) Robertson, R. E. *J. Chem. Phys.* **1966**, *44*, 3950–3956.
- (14) Argon, A. S. *Philos. Mag.* **1973**, *28*, 839–865.
- (15) Crist, B. In Howard, R. N.; Young, R. J., Eds.; *The Physics of Glassy Polymers*; Chapman & Hall: London, 1997; p 155.
- (16) Stachurski, Z. H. *Prog. Polym. Sci.* **1997**, *22*, 407–474.
- (17) Haward, R. N.; Thackray, G. *Proc. R. Soc. London, A* **1968**, *302*, 453–472.
- (18) Jho, J. Cooperative molecular motion in bisphenol-A polycarbonate. Ph.D. Thesis, The University of Michigan, Ann Arbor, 1990.
- (19) Young, R. J.; Lovell, P. A. *Introduction to Polymers*, 2nd ed.; Chapman & Hall: London, 1996.
- (20) Yang, L. Molecular Dynamics Simulation of the Glass Transition and Deformation Behavior of Amorphous Polymers. Ph.D. Thesis, The University of Michigan, Ann Arbor, Michigan, 1997.
- (21) Fan, C. F. *Macromolecules* **1995**, *28*, 5215–5224.
- (22) Brown, N. *Mater. Sci. Eng.* **1971**, *8*, 69–73.
- (23) Struik, L. C. E. *J. Non-Cryst. Solids* **1991**, *131–133*, 395–407.
- (24) Song, M.; Hourston, D. J.; Pollock, H. M. *J. Appl. Polym. Sci.* **1996**, *59*, 173–178.
- (25) Vincent, P. I. *Polymer* **1960**, *1*, 7.
- (26) Brown, N.; Ward, I. M. *J. Polym. Sci., Part A2* **1968**, *6*, 607.
- (27) Argon, A. S.; Bessonov, M. I. *Philos. Mag.* **1977**, *35*, 917–933.
- (28) Haward, R. N.; et al. *Colloid Polym. Sci.* **1980**, *258*, 643–662.
- (29) Brown, D.; Clarke, J. H. R. *Macromolecules* **1991**, *24*, 2075–2082.
- (30) McKechnie, J. I.; Haward, R. N.; Brown, D.; Clarke, J. H. R. *Macromolecules* **1993**, *26*, 198–202.
- (31) Kemmish, D. J.; Hay, J. N. *Polymer* **1985**, *26*, 905–912.
- (32) Capodanno, V.; Petrillo, E.; Romano, G.; Russo, R.; Vittoria, V. *J. Appl. Polym. Sci.* **1997**, *65*, 2635–2641.
- (33) Aref-Azar, A.; Biddlestone, F.; Hay, J. N.; Haward, R. N. *Polymer* **1983**, *24*, 1245–1251.
- (34) Ito, E.; Yamamoto, K.; Kobayashi, Y.; Hatakeyama, T. *Polymer* **1978**, *19*, 39–42.
- (35) Garcia, D. In *Proceedings of the 12th North American Thermal Analysis Society Conference*, 1983; p 256.
- (36) Bubeck, R. A.; Bales, S. E. *Polym. Eng. Sci.* **1984**, *24*, 1142–1148.
- (37) Struik, L. C. E. *Physical Aging in Amorphous Polymers and Other Materials*; Elsevier: Amsterdam, 1978.
- (38) G'Sell, C.; Hiver, J. M.; Dahoun, A.; Souahi, A. *J. Mater. Sci.* **1992**, *27*, 5031–5039.
- (39) Boyce, M. C.; Arruda, E. M.; Jayachandran, R. *Polym. Eng. Sci.* **1994**, *34*, 716–725.
- (40) Howard, R. N.; Young, R. J., Eds.; *The Physics of Glassy Polymers*; Chapman & Hall: London, 1997.
- (41) Haward, R. N. *Macromolecules* **1993**, *26*, 5860–5869.
- (42) van Melik, H. G. H.; Bressers, O. F. J. T.; den Toonder, J. M. J.; Govaert, L. E.; Meijer, H. E. H. *Polymer* **2003**, *44*, 2481–2491.

MA0489568